ACS Catalysis

Article

Dearomatization and Functionalization of Terpyridine Ligands Leading to Unprecedented Zwitterionic Meisenheimer Aluminum Complexes and Their Use in Catalytic Hydroboration

Guoqi Zhang, Jing Wu, Haisu Zeng, Michelle C Neary,
Matthew Devany, Shengping Zheng, and Pavel A. Dub

ACS Catal., **Just Accepted Manuscript** • DOI: 10.1021/acscatal.8b04096 • Publication Date (Web): 14 Dec 2018

ACS Publications

is published by the American Chemical Society. 1155 Sixteenth Street N.W., Washington, DC 20036

Dearomatization and Functionalization of Terpyridine Ligands Leading to Unprecedented Zwitterionic Meisenheimer Aluminum Complexes and Their Use in Catalytic Hydroboration

Guoqi Zhang,[1,*] Jing Wu,[1,2] Haisu Zeng,[1,2] Michelle C. Neary,[2] Matthew Devany,[2] Shengping Zheng,[2,*] and Pavel A. Dub[3,*]

[1]Department of Sciences, John Jay College and PhD in Chemistry Program, The Graduate Center of City University of New York, New York, 10019, New York, United States.

[2]Department of Chemistry, Hunter College, City University of New York, New York, 10065, New York, United States.

[3]Los Alamos National Laboratory, Los Alamos, New Mexico 87545, United States.

*Correspondence to: guzhang@jjay.cuny.edu; szh0007@hunter.cuny.edu; pdub@lanl.gov.

Abstract: This paper reports the first example of dearomatization of ubiquitous terpyridine (tpy) ligands via 2′/6′-, 3′/5′- or 4′-selective alkylation of the central pyridine ring. The reaction is mediated by the most abundant metal in the Earth's crust, aluminum (Al), and depending on the conditions employed, exhibits ionic or radical character as suggested by experimental and computational analysis. In the latter case, intermediate formation of an Al^{III} complex supported by π-radical monoanionic ligand $(tpy\cdot)^{1-}$ is apparent. The 3′/5′-alkylation leads to unprecedented zwitterionic Meisenheimer Al^{III} complexes in which the ligands are *both* redox- and chemically non-innocent. These isolable compounds were identified as efficient precatalysts for the selective hydroboration of C=O and C≡C functionalities. Turnover numbers (TONs) up to ~1000 place the corresponding complexes in the category of the most efficient Al catalysts reported to date for the title reaction. The acquired data suggests that aluminum monohydrides, or more-likely dihydrides, are relevant catalytic species.

Keywords: terpyridine • aluminum • dearomatization • hydroboration • alkynes • redox non-innocent • ligand radical

Introduction.

Homogeneous catalysis with transition metal complexes is an integral part of the scientific-technological revolution in the 20th century.[1] The properties of these complexes are the result of the interactions between the metal center and its surrounding ligands. Not only do these ligands contribute to the electronic and steric properties of the metal center, but they can even be directly involved in the catalytic reaction. Examples include cleaving or forming bonds, gaining or losing electrons and stabilizing transition states via non-covalent interactions.[2] The last decade of homogeneous catalysis was marked by an extensive development and effective use of transition metal complexes bearing so-called "redox non-innocent" ligands.[3] Catalysis with complexes containing these ligands relies on the ligand accepting/releasing electrons or forming/breaking chemical bonds of a substrate with the help of the ligand radical.[2c, 3c] The tridentate ligand 2,2′:6′,2"-terpyridine (tpy) along with its 4′-substituted (Xtpy) analogues[4] are some of the most widely used "redox-active" ligands, as shown in Fig. 1.[5]

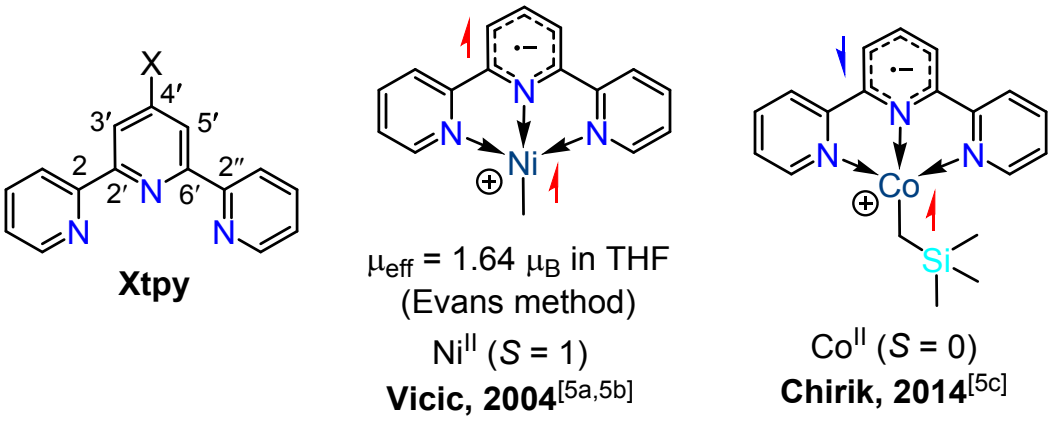

Figure 1. Structure and nomenclature for the Xtpy ligand and examples of isolable complexes based on the π-radical monoanionic ligand $(tpy\cdot)^{1-}$. Red arrows: α-spin electron; blue arrow: β-spin electron.[5]

While many homogeneous catalysts have been developed using precious metals,[6] a rational approach is needed to design metal complexes that make use of Earth-abundant elements.[7] Over the last ten years, various structurally well-defined catalysts based on first-row transition metal elements have been developed and discussed in some reviews[7d, 8] and a *Special Issue* in *Acc. Chem. Res.* **2015**.[9] Recent demands in molecular catalysis science provoked a renaissance of studies with a non-transition metal, Al.[10] In fact, Al was among the first homogeneous catalysts to be discovered (Friedel-Crafts, 1877).[11] Until recently,[12] most applications of this metal have relied almost exclusively on the use of its halide/triflate salts (Lewis acid catalysis), rather than on catalysis with well-defined complexes. Not only is Al the

most abundant metal in the Earth′s crust (8%), it is also inexpensive and much less toxic than heavy metals, which could make it ideal for applications in catalysis.[10a] The results presented in this work were obtained serendipitously as a result of our initial goal to investigate possible catalytic activity of putative Al^{III} complexes based on redox non-innocent Xtpy ligands.[13]

Results and Discussion.

In an attempt to prepare complex **1**, which would contain a one-electron reduced ligand $(Phtpy\cdot)^{1-}$, the popular precursor **L1**[14] and commercial $Al^{i}Bu_3$ were reacted under conditions (*a*) as shown in Scheme 1A. However, the reaction instead resulted in a formal 1,3-migration of one of the three ^{i}Bu groups from Al to the 2′ or 6′-position on the central pyridine ring of **L1**. The corresponding Al^{III} complex **2** was isolated in 56% yield and characterized *via* X-ray diffraction, Elem. Analysis, FTIR and solution NMR.[15] The proposed nature of the bonding of the anionic amido moiety in the "1,3-product" **2** is supported by the relatively short Al(1)–N(12) bond distance of 1.884(8) Å [1.94 Å by density functional theory (DFT) computations]. This can be compared to the dative interactions Al(1)–N(11) (2.134(8) Å) [DFT: 2.11 Å] and Al(1)–N(13) (2.132(8) Å) [DFT: 2.13 Å]. Formation of **2**, however, is not entirely unexpected. A similar dearomatization in a lutetium(III) complex has one precedent in the literature,[16] and several examples were reported for related conjugated C–N ligands such as 2,6-diiminepyridine (dimpy).[17] Inspired by these findings, the reaction conditions were further changed to (*b*) in Scheme 1 in order to prepare a putative complex similar to **2** with a $-CH_2Si(CH_3)_3$ substituent. To our further surprise, the reaction instead led to the isolation and characterization (X-ray diffraction, Elem. Analysis, FTIR and liquid NMR) of an unprecedented zwitterionic Al^{III} complex, **3**, in 55% yield, as shown in Scheme 1A.[15] By analogy with **2**, the latter can be formally viewed as a "1,4-product" of dearomatized ligand **L1** functionalized at the 3′ or 5′-position. However, in contrast to the neutral complex **2**, **3** features a zwitterionic "Meisenheimer-type" nature.[18] Meisenheimer complexes in classical organic chemistry are well-known intermediates in nucleophilic aromatic substitution, and some stable isolable examples have been reported.[18]

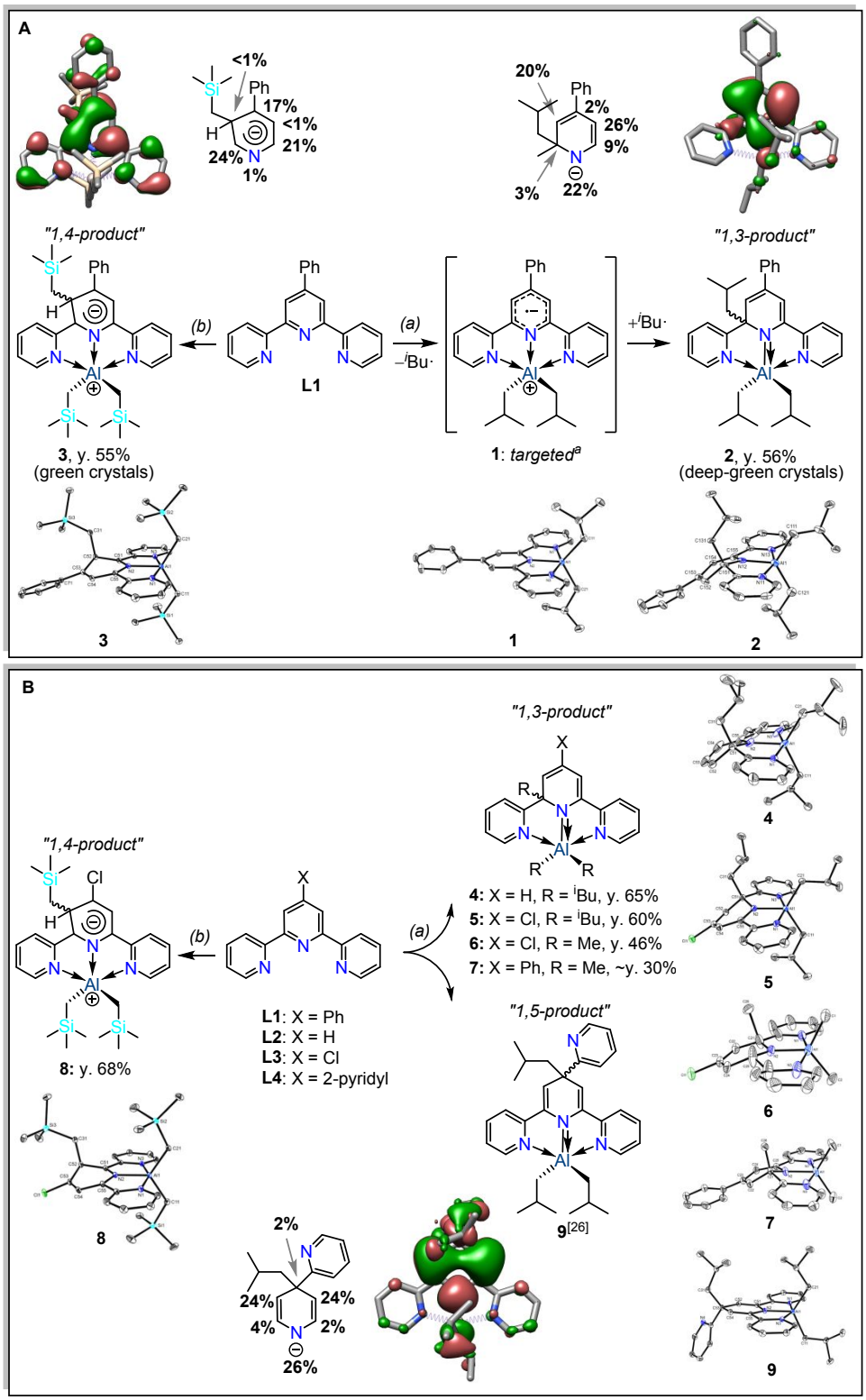

Scheme 1. Reactions of ligand **L1** with Al precursors under different conditions: (*a*) Al^{i}Bu$_3$ (1.2 eq.), Et_2O, rt, 2 h.; (*b*) (i) $AlCl_3$, THF, 24 h, rt;[19] (ii) $LiCH_2SiMe_3$, Et_2O, rt, 2 h; **B**. Scope and limitations of the reaction between various Xtpy ligands **L1–4** and commercial AlR_3 reagents under conditions (*a*) and (*b*) in **A**. X-ray structures are shown at 30% thermal ellipsoid probability level. HOMO Plots and Corresponding Atomic Contributions are Shown for the Optimized Structures of **2**, **3** and **9** Computed at the ωB97X-D/6-311++G**/SMD(diethyl ether) Level of Theory.[15] H-atoms are omitted for clarity. [a]Isolable complex **1** has not been unequivocally identified as an intermediate to formation of **2**, but the identity of the former complex is suggested by experimental and computational analyses.

Complexes of type **3** were actually predicted for the first time by Budzelaar for similar conjugated C–N imine dimpy ligands in 2006,[17a, 20] and very recently observed for the first time by Cámpora et al. for Mg/dimpy as a mixture of two isomers,[21] but this is the first example for non-imine tpy ligand. While the dative Al(1)–N(1) (2.0752(17) Å) [DFT: 2.10 Å] and Al(1)–N(3) (2.0866(17) Å) [DFT: 2.12 Å] bond lengths are similar to the analogous distances in compound **2**, the Al(1)–N(2) (1.9774(17) Å) [DFT: 2.00 Å] bond length is ~0.1 Å longer than the central Al–N bond distance for **2**. This supports the zwitterionic characterization of **3** in which the negative charge remains delocalized on the ligand. The identity of **2** and **3** as neutral and zwitterionic species, respectively, is also supported by the shapes of the computed Highest Occupied Molecular Orbitals (HOMOs) of these complexes, as shown in Scheme 1A. The liquid NMR spectra for both complexes **2** and **3** are in full agreement with the solid-state structures.[15]

Stoichiometric experiments and DFT computations have been further performed in order to explore the origin of the selective formation of "1,3-" versus "1,4-products" under conditions (*a*) and (*b*), respectively. During the work-up process for **2**, we noticed that several pieces of well-shaped green crystals spontaneously crystallized on the vial wall prior to the isolation of **2**.[15] X-ray crystallography identified these crystals to be the targeted complex **1**, which is thus either a reaction by-product or an intermediate, as shown in Scheme 1A. The ligand within complex **1** represents an anion-radical,[22] whose combination with ^{i}Bu· radical generated in the reaction mixture under conditions (*a*) may explain the formation of complex **2**. Attempts to prepare **2** in the presence of a radical trap were unsuccessful,[15] and some free ligand and complex **1** were recovered; this is consistent with the radical nature of the reaction leading to **2**. Computational analysis has been further performed to explore the reaction between **1** and ^{i}Bu· as shown in Fig. 2A.

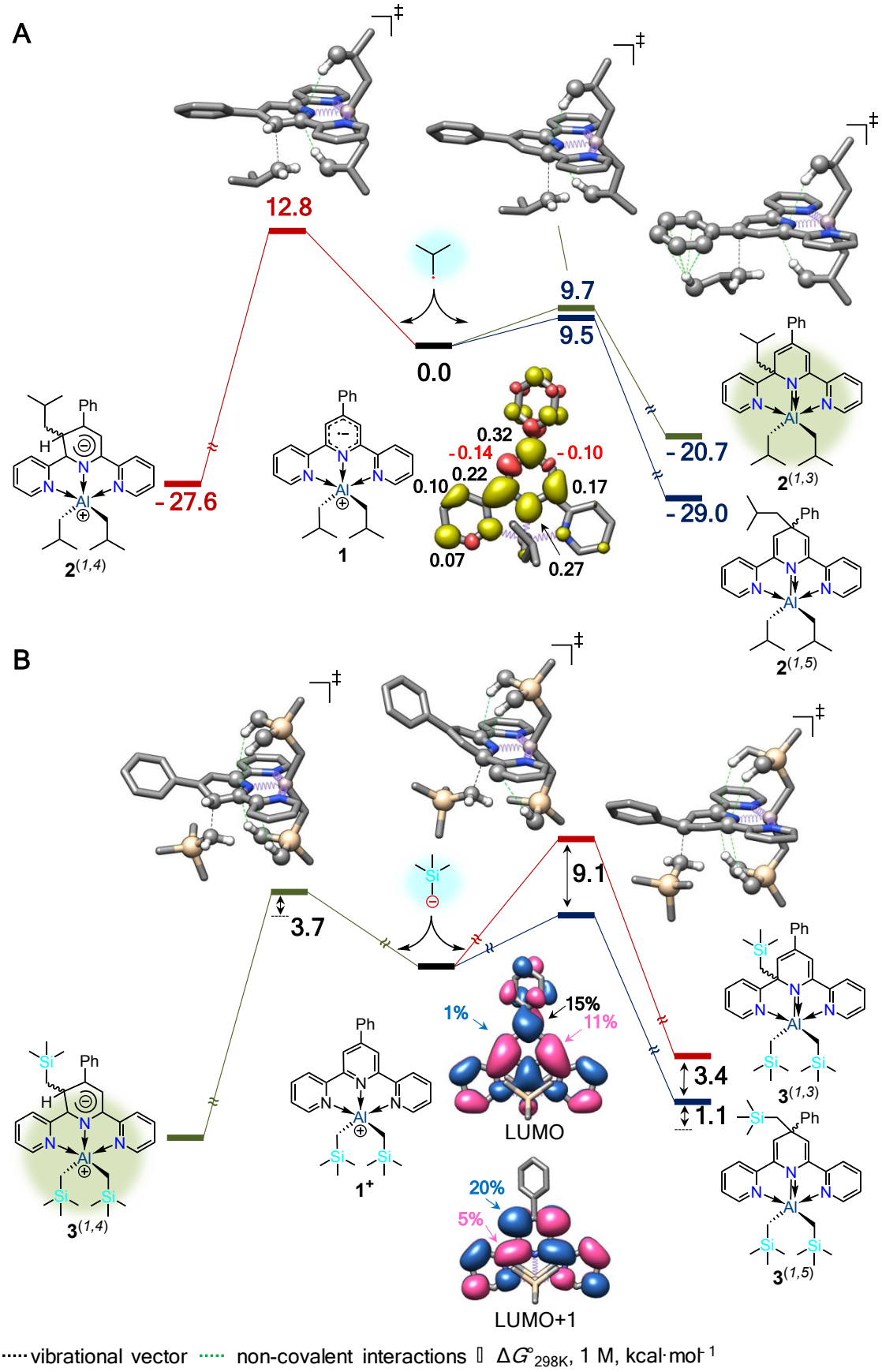

Figure 2. A. Energy Profile for the Radical Reaction Between **1**/^{i}Bu·and Mulliken Spin Density Plot for **1** (yellow: α-spin; red: β-spin); **B**. Energy Profile for the Ionic Reaction Between $\mathbf{1}^{+}$/$(CH_3)_3SiCH_2^{-}$ and LUMO/LUMO+1 Plots for $\mathbf{1}^{+}$. Computed at the ωB97X-D/6-311++G**/SMD(diethyl ether) Level of Theory (for the Optimized Structures, Non-critical H atoms are Omitted for Clarity).[23] Experimentally isolated complexes are highlighted in green.

The C–C bond formation leading to the experimentally obtained "1,3-product" **2**$^{(1,3)}$ takes place with an activation barrier of 9.7 kcal·mol^{-1} ($\Delta G°_{298K}$, 1 M). The activation barrier becomes higher (12.8 kcal·mol^{-1}) for the C–C bond formation leading to an isomeric Meisenheimer-type "1,4-product" **2**$^{(1,4)}$. This is consistent with the Mulliken spin density analysis of **1**, which has limited electron density localized on the *meta*-C atom of the central pyridine ring. Interestingly, **2**$^{(1,4)}$ is 6.9 kcal·mol^{-1} more stable than **2**$^{(1,3)}$ (or 5.8 kcal·mol^{-1} on an *E* scale). Therefore, **2**$^{(1,3)}$ is formed under kinetic control, and the reaction is irreversible due to an activation barrier of 30.4 kcal·mol^{-1} for the reverse reaction. It is also interesting to note that according to the same Mulliken spin density analysis, the unpaired electron of the redox non-innocent ligand within **1** is partially localized on the *para*-C atom of the central pyridine ring. Corresponding C–C bond formation may potentially lead to a "1,5-product" **2**$^{(1,5)}$. The latter is 8.3 kcal·mol^{-1} more stable than **2**$^{(1,3)}$ (6.1 kcal·mol^{-1} on *E* scale), and slightly more stable or even isoenergetic with **2**$^{(1,4)}$ (1.4 kcal·mol^{-1} on $G°_{298K}$ scale or 0.3 kcal·mol^{-1} on *E* scale). The activation barrier leading to **2**$^{(1,5)}$ is computed as isoenergetic with the one leading to **2**$^{(1,3)}$ ($\Delta\Delta G°_{298K} = -0.2$ kcal·mol^{-1}, $\Delta\Delta E = -0.1$ kcal·mol^{-1}). Taking into account the accuracy of DFT (at least ~3 kcal·mol^{-1})[24] and the nature of calculations themselves (conformational effects, explicit solvation, uncertainty in free energy calculations[2b]), these calculations suggest: 1) the "1,4-product" **2**$^{(1,4)}$ is likely not formed or formed in very minor quantities under conditions (*a*), and 2) along with **2**$^{(1,3)}$, one may also expect formation of the neutral "1,5-product" **2**$^{(1,5)}$. Though we did not observe **2**$^{(1,5)}$ experimentally, this might be possible by varying the nature of the tpy ligand (*e.g.* changing the substituents), Al reagent, solvent, and other conditions used for the reaction. In fact, with respect to the current reaction conditions, the relatively low isolated yield for **2**$^{(1,3)}$ (56%) does not preclude accumulation of **2**$^{(1,5)}$ in the original mixture prior to crystallization as **2**$^{(1,3)}$/**2**$^{(1,5)}$ could have very different solubility due to different molecular symmetry.

In contrast to the radical reaction we project to form **2**, we propose that **3** is formed from the reaction between **1**$^{+}$ generated in the reaction mixture[15] and the anion of $(CH_3)_3SiCH_2^-$. Similar to the **1**/^{i}Bu· radical reaction described above, one may anticipate three isomeric products **3**$^{(1,3)}$–**3**$^{(1,5)}$ as shown in Fig. 2B. The relative computed energy of these isomeric complexes is as follows: "1,4-product" ≤ "1,5-product" < "1,3-product",[25] similar to the trend for products **2**$^{(1,3)}$–**2**$^{(1,5)}$, where the "1,3-product" is clearly the least-stable one for both cases. Additionally, formation of the "1,3-product" **3**$^{(1,3)}$ needs to overcome the highest activation barrier, 5.4 kcal·mol^{-1} higher than that required for the formation of experimentally observed **3**$^{(1,4)}$. According to the analysis of Lowest Unoccupied Molecular Orbitals (LUMOs), it is

LUMO+1 that interacts with the anion of $(CH_3)_3SiCH_2^-$ leading to **3**$^{(1,4)}$. Interestingly, formation of a hypothetical "1,5-product" **3**$^{(1,5)}$ takes place with a slightly lower computed activation barrier (3.7 kcal·mol^{-1}, or 3.2 kcal·mol^{-1} on *E* scale) than the one leading to **3**$^{(1,4)}$ and this happens as a result of the interaction between LUMO and the anion of $(CH_3)_3SiCH_2^-$. The energy difference between transition states (TSs) leading to **3**$^{(1,4)}$ and **3**$^{(1,5)}$ is, however, within DFT noise. In addition, as discussed above, conformational effects, explicit solvation and other factors could have dramatic effects in tuning the energy difference between the corresponding TSs in favor of the formation of **3**$^{(1,4)}$. Similar to the radical reaction described above, relatively low isolated yield for **3**$^{(1,4)}$ (55%) does not preclude accumulation of **3**$^{(1,5)}$ in the original mixture prior to crystallization as **3**$^{(1,4)}$/**3**$^{(1,5)}$ could also have very different solubility due to different molecular symmetry. To conclude, computations about the ionic reaction between **1**$^+$/$(CH_3)_3SiCH_2^-$ suggest that the "1,3-product" is likely not formed, whereas one may anticipate the formation of a "1,5-type" product in addition to the experimentally observed "1,4-type" zwitterionic product by changing the reaction conditions discussed above.

To explore the scope and limitations of the reactions shown in Scheme 1, we further tested various commercially available Xtpy ligands **L1–4** and AlR_3 reagents under conditions (*a*) or (*b*), respectively, as shown in Scheme 1B. Various "1,3-type" **4–7** or "1,4-type" products **8** were isolated in appreciable yields between ~30–68% and fully characterized by IR, solution NMR spectroscopies, elemental analysis and X-ray crystallography.[15] Interestingly, in the reaction of Al^iBu_3 with **L4**, one of the crystals was identified as the "1,5-product" **9** based on X-ray crystallography, whereas the overall mixture is composed of two components.[26] The anionic amido moiety of **9** is suggested by the relatively short Al(1)–N(2) bond distance of 1.8967(15) Å [DFT: 1.92 Å], which is comparable to the Al–N_{amido} interaction in the "1,3-product" **2** (*vide supra*). In contrast, the dative Al–N bond lengths in **9** are 2.1012(15) [DFT: 2.14 Å] and 2.1026(15) Å [DFT: 2.15 Å], *i.e.* nicely comparable to those found in **2** and **3**, respectively. The identity of **9** as a neutral species is also supported by the shape of the computed HOMO as shown in Scheme 1B. Experimental isolation of **9** further supports our conclusions gleaned from the computational analysis that "1,5-type" products can be potentially obtained and isolated in these reactions.

The five-coordinate zwitterionic Meisenheimer Al^{III} complex **8** was further tested in the catalytic hydroboration of acetophenone and phenylacetylene with freshly distilled pinacolborane (HBpin), as shown in Scheme 2A and Scheme 3A, respectively.

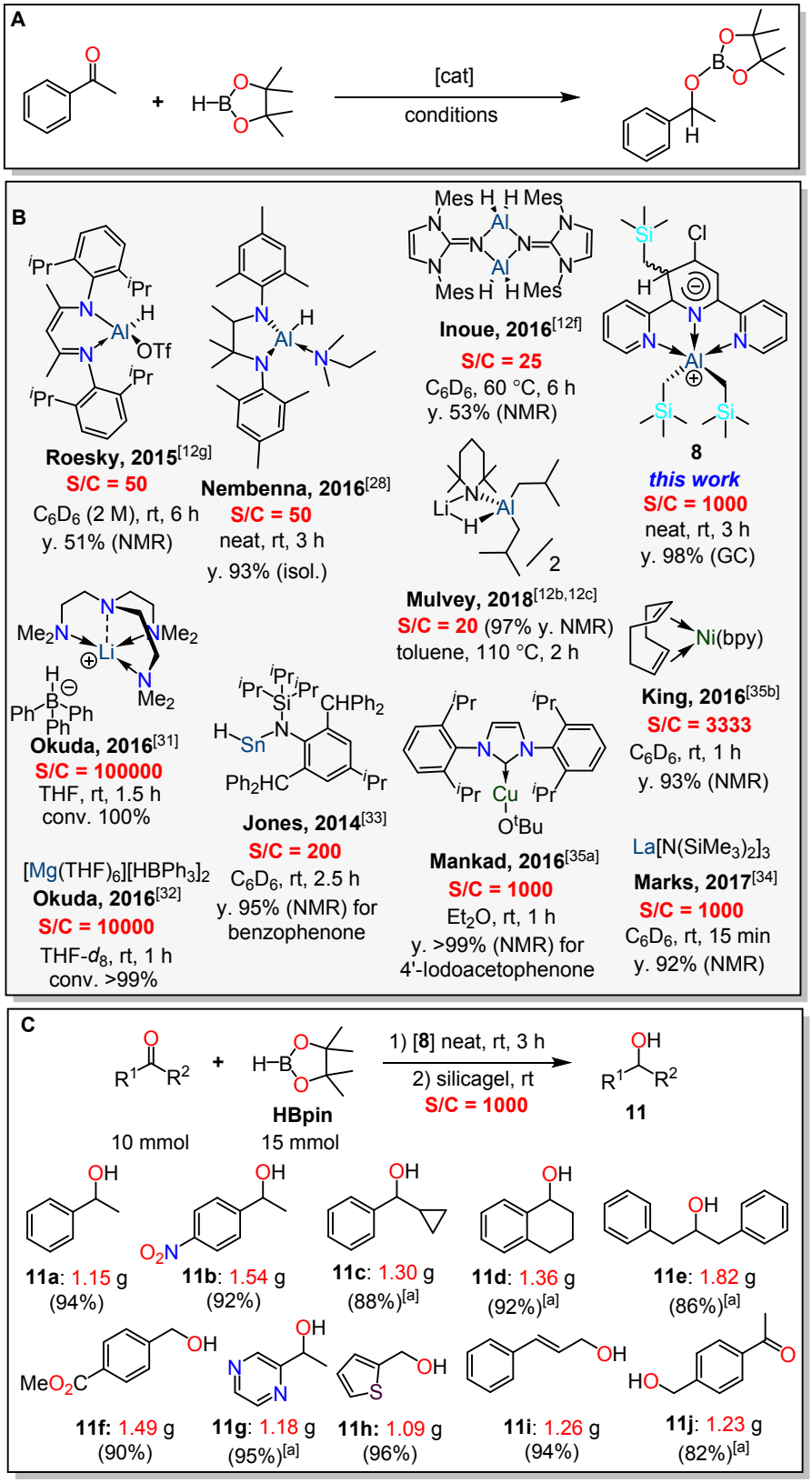

Scheme 2. **A**. Hydroboration of acetophenone with HBpin; **B**. Comparison of catalytic efficiencies of precatalyst **8** with selected, most efficient examples for reaction in **A** catalyzed by alkali, alkaline–earth, main-group, lanthanide and transition metals; **C**. Functionalized ketone hydroboration with **8**. [a] Reaction run for 16 h. S/C = substrate-to-catalyst ratio.

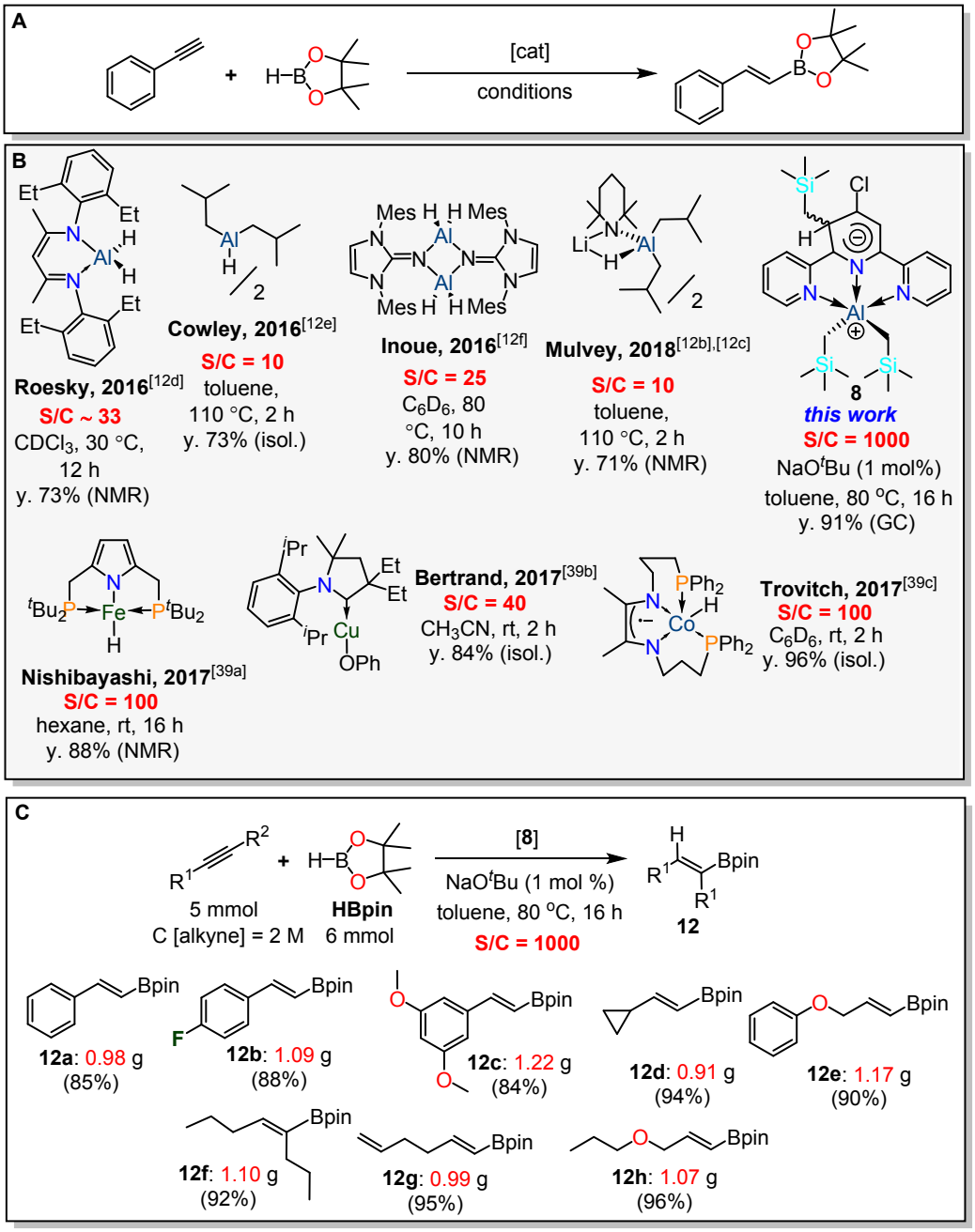

Scheme 3. A. *cis*-Selective *anti*-Markovnikov hydroboration of phenylacetylene with HBpin; **B**. All reported examples of aluminum-catalyzed and select recent examples for transition metal-catalyzed transformation in **A**; **C**. Functionalized alkyne hydroboration with **8.** S/C = substrate-to-catalyst ratio.

Ketones and alkynes are important raw materials, and their hydroboration (or dehydrogenative borylation of terminal alkynes) represents a powerful method to generate boric and boronic esters (vinylboronates or alkynylboronates), respectively. These hydroboration products are versatile building blocks in the synthesis of fine chemicals in pharmaceutical, material, and agrochemical industries.[27] Over the last five decades, various uncatalyzed, base- and acid-catalyzed, and metal-catalyzed (alkali, alkaline–earth, main-group, lanthanide and transition-metals) reactions have been reported using Brown's catecholborane

and Knochel's more robust HBpin reagents.[27] The need to access boric and boronic esters of many differing substitution patterns, stereochemistries, and functional groups has triggered the development of well-defined molecular catalysts, typically based on transition metal complexes.

Pioneering studies by Roesky[12g] and others[12b, 12c, 12f, 28] represent the only few examples, to the best of our knowledge, of aluminum-catalyzed ketone/aldehydes hydroboration. These catalysts are shown in Scheme 2B and feature turnover numbers (TONs)[29] of up to ~50 for ketones as substrates. Zwitterionic Meisenheimer complex **8** was found to catalyze the hydroboration of acetophenone producing the final product with >98% yield and a TON of 980 under neat conditions after 3 h at rt (Scheme 2B).[30] While the catalytic efficiency is lower than the most efficient examples of alkali,[31] alkaline–earth,[32] main-group,[33] lanthanide[34] and transition-metal[35] catalysts, it is comparable to others and outperforms all reported Al catalysts (Scheme 2B).

Further evaluation of the catalytic activity of **8** has been conducted on the catalytic hydroboration of phenylacetylene with HBpin.[36,37] A diversity of products in catalytic hydroboration of phenylacetylene is expected,[38] and the *cis*-selective *anti*-Markovnikov hydroboration represents one possibility as shown in Scheme 3A. We found that **8** catalyzes *cis*-selective *anti*-Markovnikov hydroboration of phenylacetylene with appreciable TON of 910 as shown in Scheme 3B. This can be compared to TONs of ~10–33 reported for all other Al catalysts,[12b, 12d-f] as well as TONs of ~40–100 for some recently reported first row transition metals (Scheme 3B).[39] In order to evaluate the scope and selectivity, various functionalized ketones/aldehydes and alkynes were hydroborated with HBpin in the presence of zwitterionic Meisenheimer Al complex **8**, as shown in Schemes 2C and 3C. All the reactions were performed on a 5–10 mmol (gram) scale to demonstrate the potential practical utility of zwitterionic Meisenheimer Al complex **8**. For both reaction types, the catalyst features excellent selectivities, leaving C=C of alkenes and arenes, CO_2Me, NO_2 and C=N functional groups unaffected. All the products, secondary alcohols and vinylboronates as a result of *anti*-Markovnikov *cis*-addition, were isolated in 84–96 % yield after column chromatography.[15]

Intrigued by the impressive catalytic activity of precatalyst **8** in the hydroboration of ketones and internal/terminal alkynes,[40] preliminary stoichiometric NMR experiments and parallel computational analyses have been performed in order to elucidate the catalytically relevant species. No visible reaction occurs when **8** and 2 equiv. of $PhC(O)CH_3$ or PhCCH alone are treated in THF-d_8 according to the ^1H and $^{13}C\{^1H\}$ NMR within 1 hour. In contrast, the same reaction with 2 equiv. of HBpin leads to ~30% conversion of **8** into new complex **10** and $pinBCH_2Si(CH_3)_3$ in a 1:1 ratio as shown in Scheme 4.[41]

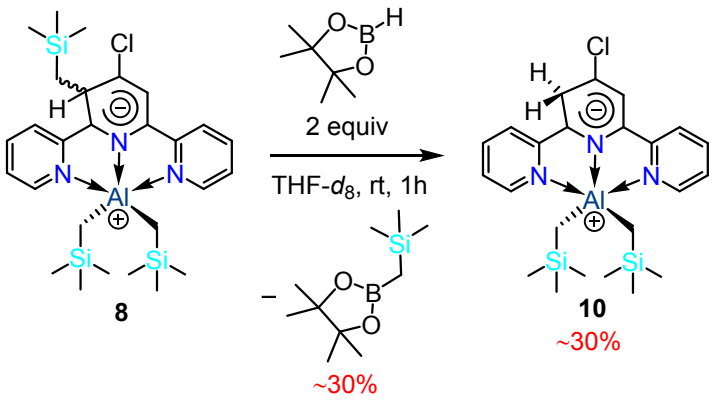

Scheme 4. Outcome of the reaction between **8** and 2 equiv. of HBpin in THF-d_8 according to the ^{1}H and ^{13}C{^{1}H} NMR spectra recorded ~1 hour after mixing the reagents ($C_{\mathbf{8}}$ ~ 0.02 M).

Several characteristic features exist in the ^{1}H NMR spectrum of **8** including the signal of the dearomatized CH proton at δ/ppm 4.50 (dd, $^3J_{HH}$ = 10 Hz, $^3J_{HH}$ = 2 Hz), and signals for two diastereotopic CH_2 protons at δ 1.03 (1H, dd, $^3J_{HH}$ = 15 Hz, $^3J_{HH}$ = 10 Hz) and 0.65 (1H, dd, $^3J_{HH}$ = 15 Hz, $^3J_{HH}$ = 2 Hz) for the $CH_2Si(CH_3)_3$ group attached to the stereogenic carbon atom of the central pyridine ring of the ligand. Additionally, four diastereotopic CH_2 protons for two $CH_2Si(CH_3)_3$ groups attached to the metal center appear as a set of second-order signals at –0.80 to –1.00 (4H).[15] For complex **10**, two dearomatized CH_2 protons are chemically equivalent and resonate at δ 2.91 (2H, s), whereas the CH_2 protons of the $CH_2Si(CH_3)_3$ groups overlap with the CH_3 protons at δ/ppm 0.00 (22H, s). The dearomatized carbon atom resonates at δ 37.7 and presumably at δ ~24 ppm (overlapped with THF-d_8) for **8** and **10**, respectively in the ^{13}C{^{1}H} NMR spectrum. The methylene carbon of the $CH_2Si(CH_3)_3$ group attached to the stereogenic carbon atom of the central pyridine ring of the ligand in **8** resonates at δ 14.3. All other C-atoms of the $CH_2Si(CH_3)_3$ groups attached to the metal center resonate in the region from δ 1 to –3 for both complexes respectively in the ^{13}C{^{1}H} NMR spectra.

Figure 3 shows the computed mechanism for the formation of **10** from **8**, as well as the free energy profile for the further putative σ-bond metathesis reaction[42] of **10** with HBpin to afford monohydride **11** and dihydride **12**. Complexes **11** and **12** can be assumed to be the likely catalytic species based on stoichiometric studies of related complexes,[43] as well as reports of Roesky,[12d, 12g] Thomas & Cowley[12a, 12e] and others.[12b, 12c, 28]

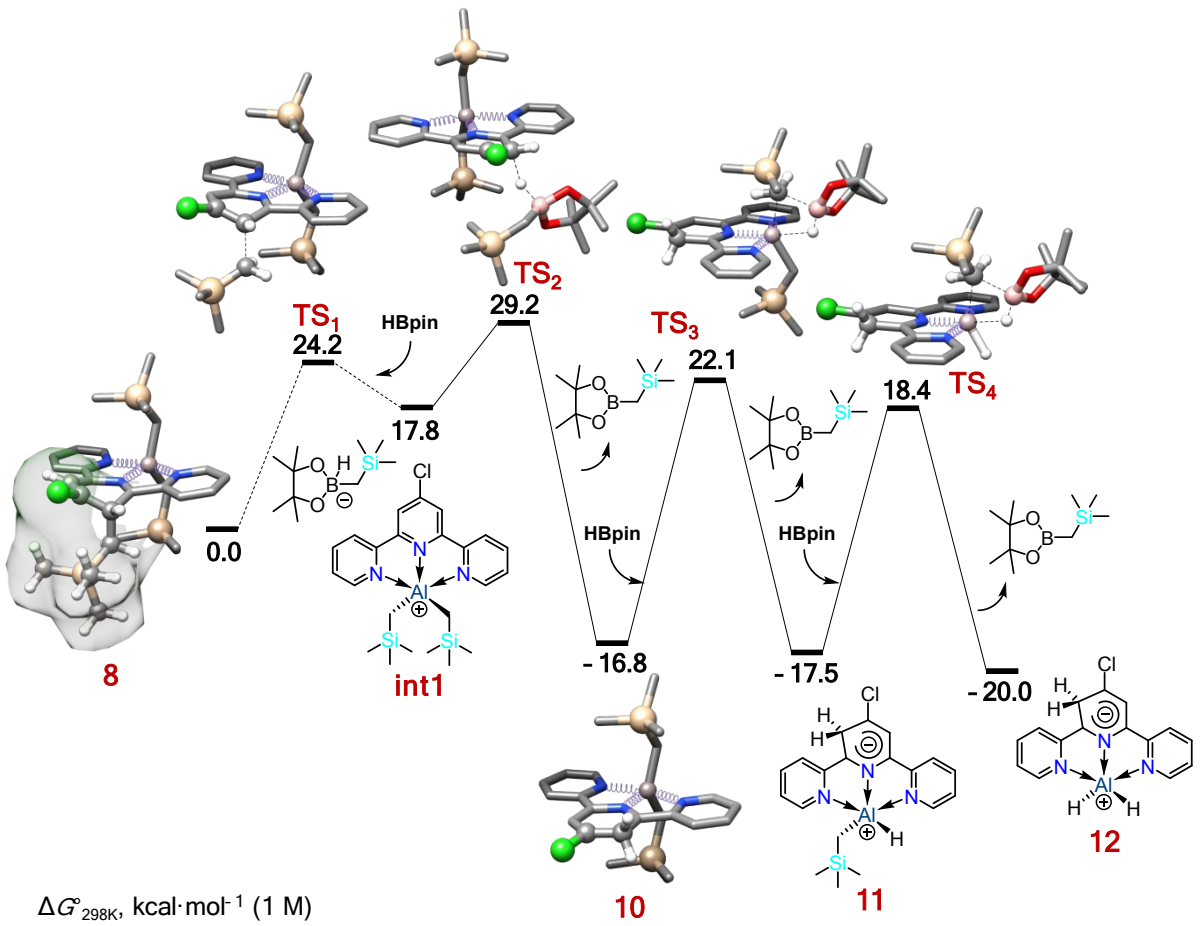

Figure 3. Computed at the ωB97X-D/6-311++G**/SMD(THF) level of theory mechanism for the formation of **10** from **8**, as well as the free energy profile for the further σ-bond metathesis reaction of **10** with HBpin to afford monohydride **11** and dihydride **12**, respectively. For the Optimized Structures, Non-critical H atoms are Omitted for Clarity. Solid line = intrinsic reaction coordinate (IRC)[44] path; dotted line = non-IRC path.

The formation of **10** from **8** takes place via a classical S_N1 mechanism.[45] Complex **10** undergoes "slow" dissociation via transition state $\mathbf{TS_1}$ to produce the $(CH_3)_3SiCH_2^-$ anion and an analog of $\mathbf{1}^+$ cation described above in Figure 2. This step is characterized by an activation barrier $\Delta G°_{298K}^{\neq}$ of 24.2 kcal·mol^{-1}. $(CH_3)_3SiCH_2^-$ further reacts with HBpin to afford the contact ion-pair complex **int1** consisting of the tetrahedral anion of $pinB(H)(CH_2Si(CH_3)_3)^-$ and the aforementioned cation, ($\Delta G°_{298K}$ = 17.8 kcal·mol^{-1}). The anion of $pinB(H)(CH_2Si(CH_3)_3)^-$ further rapidly transfers the hydride atom to the cation via low-lying $\mathbf{TS_2}$ to afford **10** and $pinBCH_2Si(CH_3)_3$ ($\Delta\Delta G°_{298K}^{\neq}$ = 11.4 kcal·mol^{-1} relative **int1**). The overall transformation **8** → **10** is very exergonic, and characterized by the $\Delta G°_{298K}$ = –16.8 kcal·mol^{-1}. Favorable formation of **10** from **8** results from a destabilization initially present in **8** due to steric constraint imposed by the bulky $(CH_3)_3SiCH_2$ group attached to the central pyridine ring. Indeed, three carbon atoms of the central pyridine ring, including the dearomatized-one, significantly deviate from the plane of the 3′/5′-functionalized tpy ligand in **8** as observed in the X-ray structure. This geometry is fully reproduced in calculations as shown in Figure 3. In

contrast, all carbon atoms of the 3′/5′-functionalized tpy ligand are planar in the optimized geometry of **10**. Finally, the step-wise reaction of **10** with two molecules of HBpin affords monohydride **11**, then dihydride **12**, along with two $pinBCH_2Si(CH_3)_3$. These steps are characterized by favorable thermodynamics of –0.7 kcal·mol^{-1} and –3.5 kcal·mol^{-1} ($\Delta\Delta G°_{298K}$ relative to **10**), respectively. The computed activation barriers of 38.9 kcal·mol^{-1} and 35.9 kcal·mol^{-1} ($\Delta\Delta G°_{298K}^{\neq}$ relative **10** and **11**), respectively, however, the values are somewhat unsettling due to their considerable magnitudes. Qualitatively, however, this is in agreement with the NMR experiment in THF-d_8 as only the partial reaction leading to **10** was observed (computed $\Delta\Delta G°_{298K}^{\neq} = 24.2$ kcal·mol^{-1} for the "slowest step"), at least within ~1h after mixing the reagents. In the catalytic reaction pool,[46] these barriers could be lowered by means of involvement of other molecules in the process (*e.g.* chemically or via specific solvation), including impurities present in substrates. Alternatively, hydrido species **11** and/or **12** could be generated via different σ-bond metathesis mechanisms, for example, via heterolytic Al–$CH_2Si(CH_3)_3$ bond dissociation following hydride transfer from the $pinB(H)(CH_2Si(CH_3)_3)^-$, obtained from association of $(CH_3)_3SiCH_2^-$ and HBpin. One can also imagine Al–$CH_2Si(CH_3)_3$ to Al–X bond substitution, where X is a better leaving group and an anionic ligand, generated from the reagents and/or impurities. This fragment can further be replaced by H leading to the hydrido species.

Based on the presently accumulated data in this work as well as works by others,[12a-e, 12g, 28, 43] and the experimental fact that both terminal and internal alkynes can be hydroborated, it is reasonable to propose the plausible mechanisms of ketones and alkynes *anti*-Markovnikov *cis*-selective hydroboration catalyzed by **8** as shown in Scheme 5.

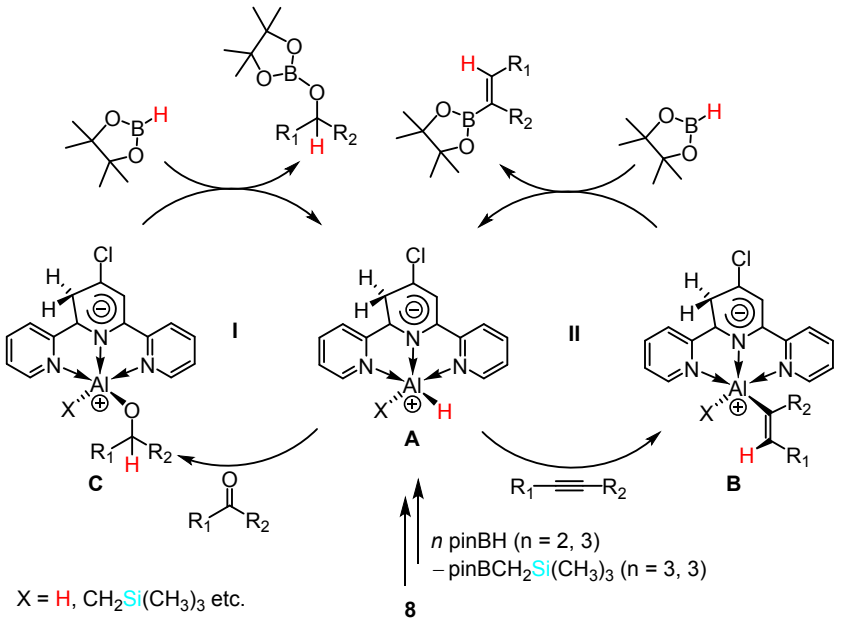

Scheme 5. Plausible mechanisms of ketones (**I**) and alkynes *anti*-Markovnikov *cis*-selective (**II**) hydroboration catalyzed by **8**. The active species are monohydride and/or more-likely dihydride complex **A**, obtained from the reaction of precatalyst **8** with HBpin.

For both reactions, the key intermediate is the mono-hydrido, or most-likely dihydrido complex **A**, obtained from **8** and HBpin as discussed above. For ketone hydroboration (catalytic cycle I), inner- or outer-sphere hydride transfer[47] from **A** to a ketone would afford alkoxo species **C** as an active intermediate or an off-loop species. Further reaction with HBpin via σ-bond metathesis or other mechanism would regenerate **A** and produce the reaction product. For alkyne hydroboration (catalytic cycle II), the first step is hydroalumination[27e] yielding alkenyl species **B**. **B** then reacts with HBpin via σ-bond metathesis or an alternative mechanism to produce the *anti*-Markovnikov *cis*-addition product and regenerate **A**. In summary, unprecedented catalytic activity of aluminum precatalyst **8** seems to be attributed to its unusual electronic and structural properties. The Meisenheimer-type anionic ligand is simultaneously both redox and chemically non-innocent. Overall the ligand seems to increase the positive charge at the aluminum center, which implies a strong Lewis acidic character. A detailed investigation of the nature of *bona fide* catalytic species, effects of the ligand, and catalytic reaction mechanisms for these two reactions is warranted in the future.[48]

Conclusions.

We report the unprecedented selective dearomatization of popular terpyridine (tpy) ligands via alkylation at various (2′/6′ vs 3′/5′ and 4′) positions of the central pyridine ring mediated by Al^{III}. Although dearomatization and 2′-functionalization of Xtpy ligands has one precedent in the literature,[16] and similar dearomatizations are reported for dimpy or related imine ligands by Budzelaar, Cámpora, van Koten and others,[17, 21, 49] this work demonstrates the first example of dearomatization and functionalization of Xtpy at 3′/5′ or 4′-positions, respectively. Experimental and computational analysis suggest that the nature of these reactions depends on the conditions used, and ionic or radical mechanisms are possible. In the latter case the reactions seems to take place via intermediate formation of complexes supported by π-radical monoanionic ligands $(Xtpy\cdot)^{1-}$. The 3′/5′-functionalized/dearomatized Xtpy ligands leading to a zwitterionic Meisenheimer complexes are of particular interest due to their unusual structures. Indeed, structure is often a key component of a molecular catalyst's design, responsible for achieving high selectivities and turnover efficiencies. Studies in this work indicate that the zwitterionic Meisenheimer complex **8** in particular is an efficient precatalyst in the selective hydroboration of ketones and alkynes with pinacolborane with a turnover number of ~1000, placing the title complexes in the category of the most efficient Al catalysts developed to date for catalytic hydroboration. Preliminary investigations suggest that precatalyst **8** undergoes reaction with HBpin to afford thermodynamically more stable Meisenheimer complex **10**,

which ultimately yields possible relevant catalytic species, the aluminum(III) monohydride or more likely dihydride complexes supported by *both* chemically and redox non-innocent ligands.

ASSOCIATED CONTENT

Supporting Information. Syntheses, characterizations, NMR spectra/charts, X-ray data for all complexes reported in this work, catalytic experiments, stoichiometric NMR experiments, computational details, three orthogonal views of HOMO's for complexes **2**, **3** and **9** as well as other details see SI. Metrical parameters for the solid-state structures are available free of charge from the Cambridge Crystallographic Data Centre under the reference numbers CCDC 1833905 (**1**), 1833906 (**2**), 1585885 (**3**), 1833907 (**4**), 1833909 (**5**), 1833908 (**6**), 1833910 (**7**), 1585884 (**8**), 1833911 (**9**) and 1834247 ([(**L3**)Al$(H_2O)_3$]$Cl_3(H_2O)_4$).

ACKNOWLEDGMENT

We are grateful to donors of the American Chemical Society Petroleum Research Fund for partial support of this work (54247-UNI3). We also acknowledge the support from the CUNY Collaborative Research Incentive Program, the PSC-CUNY awards (60328-0048) and the Seed grant from the Office for Advancement of Research at John Jay College. Partial support from the National Science Foundation (CHE-1464543) is also gratefully acknowledged. Computations were performed by using Darwin Computational Cluster (LANL).

REFERENCES

(1) Temkin, O. N., *Homogeneous Catalysis with Metal Complexes: Kinetic Aspects and Mechanisms*. Wiley: 2012; p 830.

(2) (a) Dub, P. A.; Gordon, J. C. The role of the metal-bound N–H functionality in Noyori-type molecular catalysts. *Nat. Rev. Chem.* **2018**, *2*, 396–408. (b) Dub, P. A.; Gordon, J. C. Metal–Ligand Bifunctional Catalysis: The "Accepted" Mechanism, the Issue of Concertedness, and the Function of the Ligand in Catalytic Cycles Involving Hydrogen Atoms. *ACS Catal.* **2017**, 6635-6655. (c) de Bruin, B.; Gualco, P.; Paul, N. D. In *Ligand Design in Metal Chemistry*, Stradiotto, M., Lundgren, R. J., Eds. John Wiley & Sons, Ltd: 2016; pp 176-204.

(3) (a) van der Vlugt, J. I. In *Pincer Compounds*, Morales-Morales, D., Ed. Elsevier: 2018; pp 599-621. (b) Berben, L. A.; de Bruin, B.; Heyduk, A. F. Non-innocent ligands. *Chem. Commun.* **2015**, *51*, 1553-1554. (c) Lyaskovskyy, V.; de Bruin, B. Redox Non-Innocent Ligands: Versatile New Tools to Control Catalytic Reactions. *ACS Catal.* **2012**, *2*, 270-279. (d) Caulton, K. G. Systematics and Future Projections Concerning Redox-Noninnocent Amide/Imine Ligands. *Eur. J. Inorg. Chem.* **2012**, *2012*, 435-443. (e) Chirik, P. J. Preface: Forum on Redox-Active Ligands. *Inorg. Chem.* **2011**, *50*, 9737-9740. (f) Chirik, P. J.; Wieghardt, K. Radical Ligands Confer Nobility on Base-Metal Catalysts. *Science* **2010**, *327*,

794-795. (g) Butin, K. P.; Beloglazkina, E., K.; Zyk, N., V. Metal complexes with non-innocent ligands. *Russ. Chem. Rev.* **2005**, *74*, 531.

(4) Cargill Thompson, A. M. W. The synthesis of 2,2:6,2″-terpyridine ligands – versatile building blocks for supramolecular chemistry. *Coord. Chem. Rev.* **1997**, *160*, 1-52.

(5) (a) Anderson, T. J.; Jones, G. D.; Vicic, D. A. Evidence for a Ni^{I} Active Species in the Catalytic Cross-Coupling of Alkyl Electrophiles. *J. Am. Chem. Soc.* **2004**, *126*, 8100-8101. (b) Jones, G. D.; Martin, J. L.; McFarland, C.; Allen, O. R.; Hall, R. E.; Haley, A. D.; Brandon, R. J.; Konovalova, T.; Desrochers, P. J.; Pulay, P.; Vicic, D. A. Ligand Redox Effects in the Synthesis, Electronic Structure, and Reactivity of an Alkyl−Alkyl Cross-Coupling Catalyst. *J. Am. Chem. Soc.* **2006**, *128*, 13175-13183. (c) Palmer, W. N.; Diao, T.; Pappas, I.; Chirik, P. J. High-Activity Cobalt Catalysts for Alkene Hydroboration with Electronically Responsive Terpyridine and α-Diimine Ligands. *ACS Catal.* **2015**, *5*, 622-626.

(6) Cornils, B.; Herrmann, W. A.; Beller, M.; Paciello, R., *Applied Homogeneous Catalysis with Organometallic Compounds: A Comprehensive Handbook in Four Volumes, Third Edition*. Wiley-VCH Verlag GmbH & Co. KGaA: 2017.

(7) (a) Friedfeld, M. R.; Zhong, H.; Ruck, R. T.; Shevlin, M.; Chirik, P. J. Cobalt-catalyzed asymmetric hydrogenation of enamides enabled by single-electron reduction. *Science* **2018**, *360*, 888-893. (b) Bullock, R. M. Reaction: Earth-Abundant Metal Catalysts for Energy Conversions. *Chem* **2017**, *2*, 444-446. (c) Korstanje, T. J.; van der Vlugt, J. I.; Elsevier, C. J.; de Bruin, B. Hydrogenation of carboxylic acids with a homogeneous cobalt catalyst. *Science* **2015**, *350*, 298-302. (d) Bullock, R. M. Abundant Metals Give Precious Hydrogenation Performance. *Science* **2013**, *342*, 1054-1055. (e) Zuo, W.; Lough, A. J.; Li, Y. F.; Morris, R. H. Amine(imine)diphosphine Iron Catalysts for Asymmetric Transfer Hydrogenation of Ketones and Imines. *Science* **2013**, *342*, 1080-1083. (f) Friedfeld, M. R.; Shevlin, M.; Hoyt, J. M.; Krska, S. W.; Tudge, M. T.; Chirik, P. J. Cobalt Precursors for High-Throughput Discovery of Base Metal Asymmetric Alkene Hydrogenation Catalysts. *Science* **2013**, *342*, 1076-1080. (g) Jagadeesh, R. V.; Surkus, A.-E.; Junge, H.; Pohl, M.-M.; Radnik, J.; Rabeah, J.; Huan, H.; Schünemann, V.; Brückner, A.; Beller, M. Nanoscale Fe_2O_3-Based Catalysts for Selective Hydrogenation of Nitroarenes to Anilines. *Science* **2013**, *342*, 1073-1076.

(8) (a) Hayler, J. D.; Leahy, D. K.; Simmons, E. M. A Pharmaceutical Industry Perspective on Sustainable Metal Catalysis. *Organometallics* **2018**, Article ASAP DOI: 10.1021/acs.organomet.8b00566. (b) Thomas, Z.; Robert, L. From Ruthenium to Iron and Manganese–A Mechanistic View on Challenges and Design Principles of Base–Metal Hydrogenation Catalysts. *ChemCatChem* **2018**, *10*, 1930-1940. (c) Filonenko, G. A.; van Putten, R.; Hensen, E. J. M.; Pidko, E. A. Catalytic (de)hydrogenation promoted by non-precious metals - Co, Fe and Mn: recent advances in an emerging field. *Chem. Soc. Rev.* **2018**, *47*, 1459-1483. (d) Zweig, J. E.; Kim, D. E.; Newhouse, T. R. Methods Utilizing First-Row Transition Metals in Natural Product Total Synthesis. *Chem. Rev.* **2017**, *117*, 11680-11752. (e) Morris, R. H. Iron Group Hydrides in Noyori Bifunctional Catalysis. *Chem. Rec.* **2016**, *16*, 2644-2658. (f) van der Vlugt, J. I. Cooperative Catalysis with First–Row Late Transition Metals. *Eur. J. Inorg. Chem.* **2012**, *2012*, 363-375.

(9) Chirik, P.; Morris, R. Getting Down to Earth: The Renaissance of Catalysis with Abundant Metals. *Acc. Chem. Res.* **2015**, *48*, 2495-2495.

(10) (a) Nikonov, G. I. New Tricks for an Old Dog: Aluminum Compounds as Catalysts in Reduction Chemistry. *ACS Catal.* **2017**, *7*, 7257-7266. (b) Li, W.; Ma, X.; Walawalkar, M. G.; Yang, Z.; Roesky, H. W. Soluble aluminum hydrides function as catalysts in deprotonation, insertion, and activation reactions. *Coord. Chem. Rev.* **2017**, *350*, 14-29. (c) Roesky, H. W. The Renaissance of Aluminum Chemistry. *Inorg. Chem.* **2004**, *43*, 7284-7293.

(11) (a) Friedel, C.; Crafts, J. M. C. R. *Hebd. Seances Acad. Sci.* **1877**, *84*, 1392; (b) Friedel, C.; Crafts, J. M. C. R. *Hebd. Seances Acad. Sci.* **1877**, *84*, 1450.

(12) (a) Bismuto, A.; Cowley, M. J.; Thomas, S. P. Aluminum-Catalyzed Hydroboration of Alkenes. *ACS Catal.* **2018**, *8*, 2001-2005. (b) Pollard, V. A.; Fuentes, M. Á.; Kennedy, A.

R.; McLellan, R.; Mulvey, R. E. Comparing Neutral (Monometallic) and Anionic (Bimetallic) Aluminum Complexes in Hydroboration Catalysis: Influences of Lithium Cooperation and Ligand Set. *Angew. Chem., Int. Ed.* **2018**, *57*, 10651-10655. (c) Pollard, V. A.; Orr, S. A.; McLellan, R.; Kennedy, A. R.; Hevia, E.; Mulvey, R. E. Lithium diamidodihydridoaluminates: bimetallic cooperativity in catalytic hydroboration and metallation applications. *Chem. Commun.* **2018**, *54*, 1233-1236. (d) Yang, Z.; Zhong, M.; Ma, X.; Nijesh, K.; De, S.; Parameswaran, P.; Roesky, H. W. An Aluminum Dihydride Working as a Catalyst in Hydroboration and Dehydrocoupling. *J. Am. Chem. Soc.* **2016**, *138*, 2548-2551. (e) Bismuto, A.; Thomas, S. P.; Cowley, M. J. Aluminum Hydride Catalyzed Hydroboration of Alkynes. *Angew. Chem., Int. Ed.* **2016**, *55*, 15356-15359. (f) Franz, D.; Sirtl, L.; Pöthig, A.; Inoue, S. Aluminum Hydrides Stabilized by N-Heterocyclic Imines as Catalysts for Hydroborations with Pinacolborane. *Z. Anorg. Allg. Chem.* **2016**, *642*, 1245-1250. (g) Yang, Z.; Zhong, M.; Ma, X.; De, S.; Anusha, C.; Parameswaran, P.; Roesky, H. W. An Aluminum Hydride That Functions like a Transition–Metal Catalyst. *Angew. Chem., Int. Ed.* **2015**, *54*, 10225-10229. (h) Myers, T. W.; Berben, L. A. Aluminum–Ligand Cooperative N–H Bond Activation and an Example of Dehydrogenative Coupling. *J. Am. Chem. Soc.* **2013**, *135*, 9988-9990. (i) Whiteoak, C. J.; Kielland, N.; Laserna, V.; Escudero-Adán, E. C.; Martin, E.; Kleij, A. W. A Powerful Aluminum Catalyst for the Synthesis of Highly Functional Organic Carbonates. *J. Am. Chem. Soc.* **2013**, *135*, 1228-1231.

(13) Berben, L. A. Catalysis by Aluminum(III) Complexes of Non-Innocent Ligands. *Chem.-Eur. J.* **2015**, *21*, 2734-2742.

(14) (a) Bezdek, M. J.; Chirik, P. J. Interconversion of Molybdenum Imido and Amido Complexes by Proton-Coupled Electron Transfer. *Angew. Chem., Int. Ed.* **2018**, *57*, 2224-2228. (b) Zhang, G.; Zeng, H.; Wu, J.; Yin, Z.; Zheng, S.; Fettinger, J. C. Highly Selective Hydroboration of Alkenes, Ketones and Aldehydes Catalyzed by a Well-Defined Manganese Complex. *Angew. Chem., Int. Ed.* **2016**, *55*, 14369-14372.

(15) For syntheses, characterizations, X-ray structures of all complexes reported in this work and other details see SI.

(16) Jantunen, K. C.; Scott, B. L.; Hay, P. J.; Gordon, J. C.; Kiplinger, J. L. Dearomatization and Functionalization of Terpyridine by Lutetium(III) Alkyl Complexes. *J. Am. Chem. Soc.* **2006**, *128*, 6322-6323.

(17) (a) Knijnenburg, Q.; Smits, J. M. M.; Budzelaar, P. H. M. Reaction of the Diimine Pyridine Ligand with Aluminum Alkyls: An Unexpectedly Complex Reaction. *Organometallics* **2006**, *25*, 1036-1046. (b) Knijnenburg, Q.; Gambarotta, S.; Budzelaar, P. H. M. Ligand-centred reactivity in diiminepyridine complexes. *Dalton Trans.* **2006**, 5442-5448. (c) Reardon, D.; Conan, F.; Gambarotta, S.; Yap, G.; Wang, Q. Life and Death of an Active Ethylene Polymerization Catalyst. Ligand Involvement in Catalyst Activation and Deactivation. Isolation and Characterization of Two Unprecedented Neutral and Anionic Vanadium(I) Alkyls. *J. Am. Chem. Soc.* **1999**, *121*, 9318-9325.

(18) Artamkina, G. A.; Egorov, M. P.; Beletskaya, I. P. Some aspects of anionic σ-complexes. *Chem. Rev.* **1982**, *82*, 427-459.

(19) The room temperature reaction between terpy ligands **L1**–**4** and $AlCl_3$ in dry THF afforded white solids after 24 h. These solids are extremely air-sensitive and insoluble in most organic solvents such as acetone, acetonitrile, chloroform and toluene, but are soluble in methanol, leading to rapid decomposition. No satisfactory elemental analysis results could be obtained. For ligand **L3** in particular, elemental analysis C 45.13%, H 3.81%, N 8.66% indicates the complicated nature of the product with a possible stoichiometry of (**L3**)$AlCl_3(THF)_n$. In a separate experiment, the white solid (20 mg) from the reaction of **L3** and anhydrous $AlCl_3$ (131.9 mg, 1.00 mmol) in dry THF in a glovebox was brought out and redissolved in MeOH (3 mL) and acetone (3 mL). The colorless solution was slowly evaporated in the air for 3 days to give colorless crystals. The crystals were then characterized by X-ray diffraction. The complex was identified as [(**L3**)$Al(H_2O)_3]Cl_3$•$(H_2O)_4$.

The white solids obtained in step (i) are directly used in the following step (ii) after a small work-up.[15]

(20) Budzelaar, P. H. M. Radical Chemistry of Iminepyridine Ligands. *Eur. J. Inorg. Chem.* **2012**, *2012*, 530-534.

(21) Sandoval, J. J.; Palma, P.; Álvarez, E.; Cámpora, J.; Rodríguez-Delgado, A. Mechanism of Alkyl Migration in Diorganomagnesium 2,6-Bis(imino)pyridine Complexes: Formation of Grignard-Type Complexes with Square-Planar Mg(II) Centers. *Organometallics* **2016**, *35*, 3197-3204.

(22) The N(1)−C(35), C(35)−C(41) and C(41)−N(2) distances of 1.355(3), 1.456(3), and 1.377(3) Å, respectively, are consistent with one electron reduction of the terpyridine chelate.[5c]

(23) On a computed *G*° profile, association of two ions $\mathbf{1}^+/(CH_3)_3SiCH_2^-$ is exergonic. For example, the transition state leading to $\mathbf{3}^{(1,2)}$ and $\mathbf{3}^{(1,2)}$ itself are computed to be –21.1 kcal·mol^{-1} and –47.5 kcal·mol^{-1} relative to "free" ions, respectively. In a solution, "free" ions do not exist (each cation and anion are strongly solvated by a solvent), and the association of two ions is expected to have some activation barrier. In order to avoid possible confusion, only relative energies are reported for the ionic reactions in Fig. 2B.

(24) Laury, M. L.; Wilson, A. K. Performance of Density Functional Theory for Second Row (4d) Transition Metal Thermochemistry. *J. Chem. Theory Comput.* **2013**, *9*, 3939-3946.

(25) Complex $\mathbf{3}^{(1,5)}$ is 1.1 kcal·mol^{-1} less stable than $\mathbf{3}^{(1,4)}$ on $G°_{298K}$ scale but 0.4 kcal·mol^{-1} more stable on *E* scale, indicating that both have similar energy.

(26) The identity of the second component in the mixture is now under investigation. Tentatively, it can be identified as a $\mathbf{9}^{(1,3)}$ product by comparing the NMR data with those of the structurally related complex **2**. This assignment is also consistent with the Energy Profile in Fig. 2A.

(27) (a) Stockland, R. A. J., Synthesis of Organoboronic Acids, Organoboronates, and Related Compounds. In *Practical Functional Group Synthesis*, John Wiley & Sons, Inc.: 2016. (b) Chong, C. C.; Kinjo, R. Catalytic Hydroboration of Carbonyl Derivatives, Imines, and Carbon Dioxide. *ACS Catal.* **2015**, *5*, 3238-3259. (c) Lennox, A. J. J.; Lloyd-Jones, G. C. Selection of boron reagents for Suzuki-Miyaura coupling. *Chem. Soc. Rev.* **2014**, *43*, 412-443. (d) Barbeyron, R.; Benedetti, E.; Cossy, J.; Vasseur, J.-J.; Arseniyadis, S.; Smietana, M. Recent developments in alkyne borylations. *Tetrahedron* **2014**, *70*, 8431-8452. (e) Trost, B. M.; Ball, Z. T. Addition of Metalloid Hydrides to Alkynes: Hydrometallation with Boron, Silicon, and Tin. *Synthesis* **2005**, *2005*, 853-887.

(28) Jakhar, V. K.; Barman, M. K.; Nembenna, S. Aluminum Monohydride Catalyzed Selective Hydroboration of Carbonyl Compounds. *Org. Lett.* **2016**, *18*, 4710-4713.

(29) Kozuch, S.; Martin, J. M. L. "Turning Over" Definitions in Catalytic Cycles. *ACS Catal.* **2012**, *2*, 2787-2794.

(30) Hydroboration of acetophenone with neutral precatalyst **5** under conditions of Scheme 3D was also tested. Only 140 turnovers were achived in contrast to the 980 with zwitterionic **8**.

(31) Mukherjee, D.; Osseili, H.; Spaniol, T. P.; Okuda, J. Alkali Metal Hydridotriphenylborates [(L)M][$HBPh_3$] (M = Li, Na, K): Chemoselective Catalysts for Carbonyl and CO_2 Hydroboration. *J. Am. Chem. Soc.* **2016**, *138*, 10790-10793.

(32) Mukherjee, D.; Shirase, S.; Spaniol, T. P.; Mashima, K.; Okuda, J. Magnesium hydridotriphenylborate [$Mg(thf)_6$][$HBPh_3$]$_2$: a versatile hydroboration catalyst. *Chem. Commun.* **2016**, *52*, 13155-13158.

(33) Hadlington, T. J.; Hermann, M.; Frenking, G.; Jones, C. Low Coordinate Germanium(II) and Tin(II) Hydride Complexes: Efficient Catalysts for the Hydroboration of Carbonyl Compounds. *J. Am. Chem. Soc.* **2014**, *136*, 3028-3031.

(34) Weidner, V. L.; Barger, C. J.; Delferro, M.; Lohr, T. L.; Marks, T. J. Rapid, Mild, and Selective Ketone and Aldehyde Hydroboration/Reduction Mediated by a Simple Lanthanide Catalyst. *ACS Catal.* **2017**, *7*, 1244-1247.

(35) (a) Bagherzadeh, S.; Mankad, N. P. Extremely efficient hydroboration of ketones and aldehydes by copper carbene catalysis. *Chem. Commun.* **2016**, *52*, 3844-3846. (b) King, A. E.; Stieber, S. C. E.; Henson, N. J.; Kozimor, S. A.; Scott, B. L.; Smythe, N. C.; Sutton, A. D.; Gordon, J. C. Ni(bpy)(cod): A Convenient Entryway into the Efficient Hydroboration of Ketones, Aldehydes, and Imines. *Eur. J. Inorg. Chem.* **2016**, *2016*, 1635-1640.

(36) The reaction required 1 mol% of NaO^{t}Bu, possibly for catalyst activation as discussed elsewhere: Docherty, J. H.; Peng, J.; Dominey, A. P.; Thomas, S. P. Activation and Discovery of Earth-Abundant Metal Catalysts Using Sodium tert-Butoxide. *Nat. Chem*. **2017**, *9*, 595-600. Separate experiments show that 1 mol% of NaO^{t}Bu also catalyzes the background reaction, but only affording the product with ~10% yield under identical conditions, in agreement with studies of Wu, Liu and Zhao.[37]

(37) Wu, Y.; Shan, C.; Ying, J.; Su, J.; Zhu, J.; Liu, L. L.; Zhao, Y. Catalytic hydroboration of aldehydes, ketones, alkynes and alkenes initiated by NaOH. *Green Chem.* **2017**, *19*, 4169-4175.

(38) Haberberger, M.; Enthaler, S. Straightforward Iron-Catalyzed Synthesis of Vinylboronates by the Hydroboration of Alkynes. *Chem. As. J.* **2013**, *8*, 50-54.

(39) (a) Nakajima, K.; Kato, T.; Nishibayashi, Y. Hydroboration of Alkynes Catalyzed by Pyrrolide-Based PNP Pincer–Iron Complexes. *Org. Lett.* **2017**, *19*, 4323-4326. (b) Romero, E. A.; Jazzar, R.; Bertrand, G. (CAAC)CuX-catalyzed hydroboration of terminal alkynes with pinacolborane directed by the X-ligand. *J. Organom. Chem.* **2017**, *829*, 11-13. (c) Ben-Daat, H.; Rock, C. L.; Flores, M.; Groy, T. L.; Bowman, A. C.; Trovitch, R. J. Hydroboration of alkynes and nitriles using an α-diimine cobalt hydride catalyst. *Chem. Commun.* **2017**, *53*, 7333-7336.

(40) Complex **8** outperforms all reported Al catalysts by at least one order of magnitude in terms of TON, see Schemes 3–4.

(41) see SI for the full description of the experiment, NMR spectra/charts and peak assignments in THF-d_8. ^{1}H NMR for **10**: δ 0.0 (s, 22H), 2.91 (s, 2H), 7.27 (m, 2H), 7.60 (m, 1H), 7.79 (dt, J = 8 Hz, J = 2 Hz, 1H), 7.85 (dt, J = 8 Hz, J = 2 Hz, 1H), 8.22 (d, J = 8 Hz, 1H), 8.37 (d, J = 8 Hz, 1H), 8.52 (d, J = 8 Hz, 1H), 8.61 (vt, 1H); ^{1}H NMR for pinBCH$_2$Si(CH$_3$)$_3$: δ 1.17 (s, 12H), –0.10 (s, 11H); ^{13}C{^{1}H} NMR for pinBCH$_2$Si(CH$_3$)$_3$: δ –1.4 (s, 3C), 23.0 (s, 1C), ~24.0 (s, 4C), 80.9 (s, 2C). Further progress of the reaction has not been studied for the present contribution.

(42) Waterman, R. σ-Bond Metathesis: A 30-Year Retrospective. *Organometallics* **2013**, *32*, 7249-7263.

(43) Espinal-Viguri, M.; Woof, C. R.; Webster, R. L. Iron-Catalyzed Hydroboration: Unlocking Reactivity through Ligand Modulation. *Chem.-Eur. J.* **2016**, *22*, 11605-11608.

(44) Maeda, S.; Harabuchi, Y.; Ono, Y.; Taketsugu, T.; Morokuma, K. Intrinsic reaction coordinate: Calculation, bifurcation, and automated search. **2015**, *115*, 258-269.

(45) S_N2 reaction between **8** and HBpin has an estimated barrier of 100 kcal·mol^{-1} according to the constrained potential energy surface scan calculations and can be ruled out at least for 1:1 reaction **8**–HBpin. The homolytic C–C bond cleavage in **8** can also be ruled out based on computations performed for similar complex **2** in Fig. 2: the gap in activation barrier for the homolytic/heterolytic C–C bond cleavage is 15.1 kcal·mol^{-1} in the favor of heterolytic one.

(46) For the definition of the term "catalytic reaction pool" see: Dub, P. A.; Gordon, J. C. The mechanism of enantioselective ketone reduction with Noyori and Noyori–Ikariya bifunctional catalysts. *Dalton Trans.* **2016**, *45*, 6756-6781.

(47) Eisenstein, O.; Crabtree, R. H. Outer sphere hydrogenation catalysis. *New J. Chem.* **2013**, *37*, 21-27.

(48) One can also imagine a mechanism in which the hydride is actually transferred to/from the redox and chemically non-innocent ligand in **10**. In such a scenario, **10** does not need to be converted to **11** or **12** via high-energy σ-bond metathesis processes.

(49) (a) Sandoval, J. J.; Álvarez, E.; Palma, P.; Rodríguez-Delgado, A.; Cámpora, J. Neutral Bis(imino)-1,4-dihydropyridinate and Cationic Bis(imino)pyridine σ-Alkylzinc(II) Complexes as Hydride Exchange Systems: Classic Organometallic Chemistry Meets Ligand-Centered, Biomimetic Reactivity. *Organometallics* **2018**, *37*, 1734-1744. (b) Nienkemper, K.; Kehr, G.; Kehr, S.; Fröhlich, R.; Erker, G. (Amidomethyl)pyridine zirconium and hafnium complexes: Synthesis and structural characterization. *J. Organom. Chem.* **2008**, *693*, 1572-1589. (c) Fedushkin, I. L.; Tishkina, A. N.; Fukin, G. K.; Hummert, M.; Schumann, H. Zinc Complexes with the Chelating Amido-Imino Ligand [1-*n*-Butyl-2-(2,6-diisopropylphenyl)iminoacenaphthen-1-yl]-2,6-diisopropylphenylamide (L): Synthesis, Molecular Structure and Reactivity of $[(L)\text{-}ZnCl]_2$, (L)Zn-nBu and $(L)ZnN(SiMe_3)_2$. *Eur. J. Inorg. Chem.* **2008**, *2008*, 483-489. (d) Cámpora, J.; Pérez, C. M.; Rodríguez-Delgado, A.; Naz, A. M.; Palma, P.; Álvarez, E. Selective Alkylation of 2,6-Diiminopyridine Ligands by Dialkylmanganese Reagents: A "One-Pot" Synthetic Methodology. *Organometallics* **2007**, *26*, 1104-1107. (e) Bailey, P. J.; Dick, C. M.; Fabre, S.; Parsons, S.; Yellowlees, L. J. Complexation of dimethylmagnesium with α-diimines; structural and EPR characterisation of single electron and alkyl transfer products. *Dalton Trans.* **2006**, 1602-1610. (f) Riollet, V.; Copéret, C.; Basset, J.-M.; Rousset, L.; Bouchu, D.; Grosvalet, L.; Perrin, M. Reaction of "$[Mn_{II}(CH_2tBu)_2]$" with Bidentate Diimine Ligands: From Simple Base Adducts to C–C Activation of the Ligand. *Angew. Chem., Int. Ed.* **2002**, *41*, 3025-3027. (g) Gibson, V. C.; Redshaw, C.; White, A. J. P.; Williams, D. J. Synthesis and structural characterisation of aluminium imino-amide and pyridyl-amide complexes: bulky monoanionic N,N chelate ligands via methyl group transfer. *J. Organom. Chem.* **1998**, *550*, 453-456. (h) Wissing, E.; Kaupp, M.; Boersma, J.; Spek, A. L.; van Koten, G. Alkylation Reactions of Dialkylzinc Compounds with 1,4-Diaza-1,3-butadienes: Cationic and Radical Anionic Organozinc Intermediates. Molecular Structure of the Cationic Organozinc Species [MeZn(tert-BuN:CHCH:N-*tert*-Bu)]O_3SCF_3 and Me_2Zn(bpy) (bpy = 2,2'-Bipyridine). *Organometallics* **1994**, *13*, 2349-2356. (i) Wissing, E.; van der Linden, S.; Rijnberg, E.; Boersma, J.; Smeets, W. J. J.; Spek, A. L.; van Koten, G. Organozinc .alpha.-Diimine Radicals, Synthesis and Reactivity toward Alkyl Halides. *Organometallics* **1994**, *13*, 2602-2608. (j) Van Koten, G.; Jastrzebski, J. T. B. H.; Vrieze, K. Stable 1,4-diaza-1,3-butadiene(α-diimine)-zinc and -aluminium radicals formed in single electron transfer reactions: their consequences for organic syntheses. *J. Organom. Chem.* **1983**, *250*, 49-61.

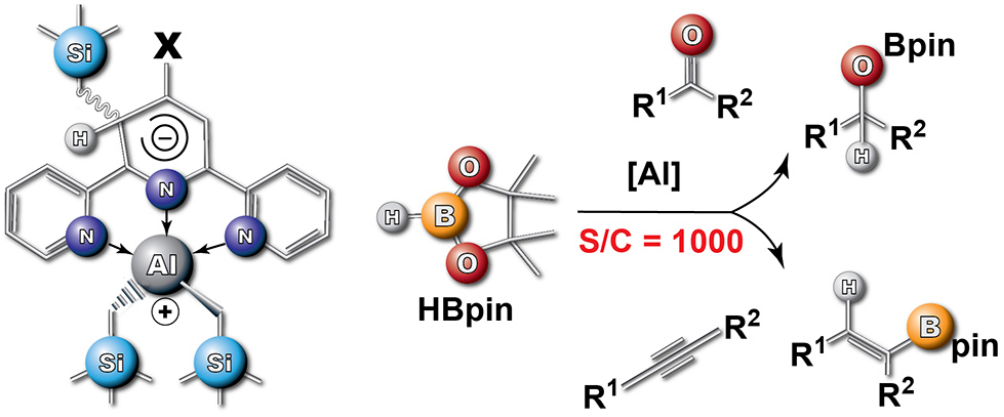

82x34mm (300 x 300 DPI)